Pergamon

0014-3057(95)00056-9

Eur. Polym. J. Vol. 31, No. 10, pp. 957–967, 1995

0014-3057/95 $9.50 + 0.00

MORPHOLOGY, MECHANICAL AND VISCOELASTIC BEHAVIOUR OF BLENDS OF NITRILE RUBBER AND ETHYLENE–VINYL ACETATE COPOLYMER

HIMA VARGHESE,[1] S. S. BHAGAWAN,[2] S. SOMESWARA RAO[2] and SABU THOMAS[1]*

[1]School of Chemical Sciences, Mahatma Gandhi University, Priyadarshini Hills P.O., Kottayam, Kerala 686 560 and [2]Propellant Engineering Division, Vikram Sarabhai Space Centre, Thiruvananthapuram, Kerala 695 022, India

(Received 11 April 1994; accepted in final form 8 September 1994)

Abstract—Nitrile rubber/ethylene–vinyl acetate copolymer (NBR/EVA) blends with different ratios were prepared by using a two roll mixing mill. The morphology of the blends was studied using optical and electron microscopies. The morphology of the blends indicated a two phase structure in which the minor phase is dispersed as domains in the major continuous phase. However, between 40 and 50 wt% of NBR content both NBR and EVA exist as continuous phases and generate a co-continuous morphology. The viscoelastic properties have been determined using a Rheovibron Viscoelastometer at 35 Hz over a wide range of temperatures. The effect of blend ratio on the mechanical properties such as tensile strength, elongation at break, stress–strain behaviour and hardness has been investigated. The mechanical properties increase with the increase of EVA content in the blend. Attempts have been made to correlate the variation of properties with morphology of the blend. Various composite models have been used to fit experimental mechanical and viscoelastic data.

INTRODUCTION

The scientific and commercial progress in the area of polymer blends during the past two decades has been tremendous and was driven by the realizations that new molecules are not always required to meet needs for new materials and that blending can be implemented more rapidly and economically than the development of new chemistry [1]. Extensive studies have been carried out in the area of polymer blends. The blends of poly(methyl methacrylate), poly(ethyl methacrylate) and poly(vinyl acetate) with poly(vinylidene fluoride), polycarbonate/poly(ϵ-caprolactone), polyethylene terephthalate/polycarbonate etc. are reported by Paul and coworkers [2–6]. Blends of poly(methyl methacrylate)/poly(styrene-co-acrylonitrile), poly(ϵ-caprolactone)/poly(styrene-co-acrylonitrile), polystyrene/poly(vinyl methyl ether), isotactic polypropylene/ethylene–propylene rubber, natural rubber/low density poly ethylene and 1,2-polybutadiene/natural rubber are also reported [7–12].

Nitrile rubber compounds (NBR) have excellent oil resistance, abrasion resistance and mechanical properties but poor ozone resistance. The oil resistance of nitrile rubber is due to the polarity of the acrylonitrile group. Nitrile rubber is highly resistant to non-polar oils and solvents. Ethylene–vinyl acetate copolymers (EVA) are random structured polymers which offer excellent ozone resistance, weather resistance and mechanical properties [13]. Several polymers have been blended with EVA and NBR to make high performance materials. The blends of EVA/silicone rubber have unique heat shrinkable characteristics, good mechanical properties and lower cost [14]. Several other blends based on EVA are also reported [15–21]. A flame resistant conveyor belting was developed from NBR/PVC blends [22]. Blends of NBR/EPDM show better oil swelling resistance [23]. Hot oil resistant blends of NBR with polyethylene and polypropylene have been developed by Coran and Patel [24]. Blending of nitrile rubber with EVA lead to a new class of materials having excellent oil resistance, ozone resistance and mechanical properties. However, no attempt has been made so far to develop blends of nitrile rubber and EVA. Recently, Thomas and coworkers have developed blends of EVA with polypropylene and natural rubber. Miscibility, morphology, crystallization, mechanical properties and ageing behaviour of these blends have been studied in detail [25–31]. Blends of NR/EVA have been successfully used for the manufacture of microcellular solings [13].

A blend morphology wherein one component is dispersed within a continuum of the other has received great attention in the literature. It has been reported that the properties of polymer blends are strongly influenced by the morphology of the system [32, 33]. Baer [33] found mechanical and dynamic properties to be dependent mainly on particle size, independent of the processing methods used. The mechanism of toughening was correlated with particle size and size distribution by Riew *et al.* [34]. Cimmino *et al.* [35] have related the mechanical properties of binary polyamide 6/rubber blends with the blend morphology. By the characterization of

*To whom all correspondence should be addressed.

blend morphology. Yang *et al.* [36] analysed the compatibility of polypropylene with ethylene–propylene diene rubber, polybutadiene rubber and styrene–butadiene rubber. A 70/30 blend of NR/PP shows a co-continuous morphology. The co-continuity exhibited in this blend composition is due to the high volume fraction of NR and low viscosity of PP compared to the other component [37]. Transmission electron microscopy was employed to identify the morphology of the poly(styrene-b-isoprene) diblock copolymer/polystyrene homopolymer blend and it was found that the morphology generated depends on the magnitude of diblock copolymer molecular weight [38]. The impact behaviour observed for iPP/EP-55 and iPP/EP-88 blend samples is explained in terms of the different mode and state of dispersion of the two copolymers in the isotactic polypropylene (iPP) matrix [39]. Scanning electron microscopy is used to study the change in morphology of NR/HDPE blends during the time of extrusion [40].

Miscibility and phase behaviour of polymer blends are of crucial importance in many applications. Miscibility in polymer blends can easily be investigated by dynamic mechanical analysis in terms of changes in T_g (glass transition temperature) of the components of the blend. Miscible blends will have a single and sharp glass transition temperature intermediate between those of the individual polymers. In the case of borderline miscibility broadening of the transition will occur whereas two separate transitions between those of the constituents may result in the case of complete immiscibility [41]. One of the main disadvantages of EVA based blends is the low maximum service temperature which is dependent on the crystalline melting point of EVA. Cyclic stressing during service generates heat and hence the study of viscoelastic behaviour of these blends become important.

In this paper we report the results of our studies on morphology, mechanical and viscoelastic properties of nitrile rubber/ethylene–vinyl acetate copolymer (NBR/EVA) blends. More specifically the influence of composition on morphology, mechanical properties and viscoelastic behaviour has been analysed. Morphology of the blends has been related to the properties. Various models such as parallel model, series model and Halpin–Tsai equation have been used to fit the experimental mechanical and viscoelastic data.

EXPERIMENTAL

Materials used

NBR (Aparene N-553NS) having 34% bound acrylonitrile content was supplied gratis by Gujarat Apar Polymers Ltd, Bombay. EVA (Pilene-1802) having 18% vinyl acetate content was procured from PIL, Madras. The basic characteristics of NBR and EVA are given in Table 1.

Preparation of blends and test samples

The blends of NBR/EVA were prepared on a two roll mixing mill having a friction ratio 1:1.4. The blends are designated as N_x ($x = 0, 10 \ldots 100$), where the value of x indicates the weight percentage of NBR in the blend. Nitrile rubber and EVA were separately masticated for 2 min. The masticated rubbers were then mixed together. The total mixing time was 7 min in all cases. The sheeted out stock was compression moulded in an electrically heated hand press at 150°C for 2 min. No significant degradation of the materials has been occurred during processing techniques. The mould was specially designed in such a way that it could be cooled immediately after moulding, keeping the samples still under compression. The samples for tensile test, dynamic mechanical analysis were punched along the mill grain direction from the moulded sheet.

Morphology studies

Moulded samples of the blend were broken after freezing the samples using liquid nitrogen. This was done to avoid any possible deformation of the phases. For studying the morphology of the blends NBR was preferentially extracted from EVA rich blends using toluene and EVA from NBR rich blends using CCl_4. From the 50/50 blend NBR was extracted. The microtomed edge of the sample was kept immersed in the solvent for about 48 hr at ambient temperature for the preferential extraction of one of the phases. The samples were then dried in an air oven at 40 ± 1°C for 24 hr. The dried samples were then preserved in a desiccator for SEM studies. The solvent extracted samples were then sputter coated with Au/Pd alloy and SEM observations were made using JEOL-JSM-T330A SEM. Morphological studies were also carried out on thin films of these blends using optical microscope.

Mechanical properties

Tensile testing of the samples was done at 25 ± 2°C according to ASTM D-412-87 test method using dumb bell shaped test pieces at a cross head speed of 500 mm/min

Table 1. Details of materials used

Materials	Characteristics	Source
Nitrile Rubber (Aparene N553NS)	Volatile matter (%): 0.130 Antioxidant (%): 1.400 Organic acid (%): 0.250 Soap (%): 0.004 Mooney viscosity, ML_{1+4} 100 C: 40.000 Bound acrylonitrile (%): 34.000 Intrinsic viscosity (dl/g): 1.527	Gujarat Apar Polymers Ltd, Bombay
Ethylene–vinyl acetate copolymer (Pilene 1802)	Melt flow index (g/10 min): 2.000 Density (g/cc): 0.937 Vicat softening point (°C): 59.000 Vinyl acetate (%): 18.000 Intrinsic viscosity (dl/g): 0.170	PIL, Madras

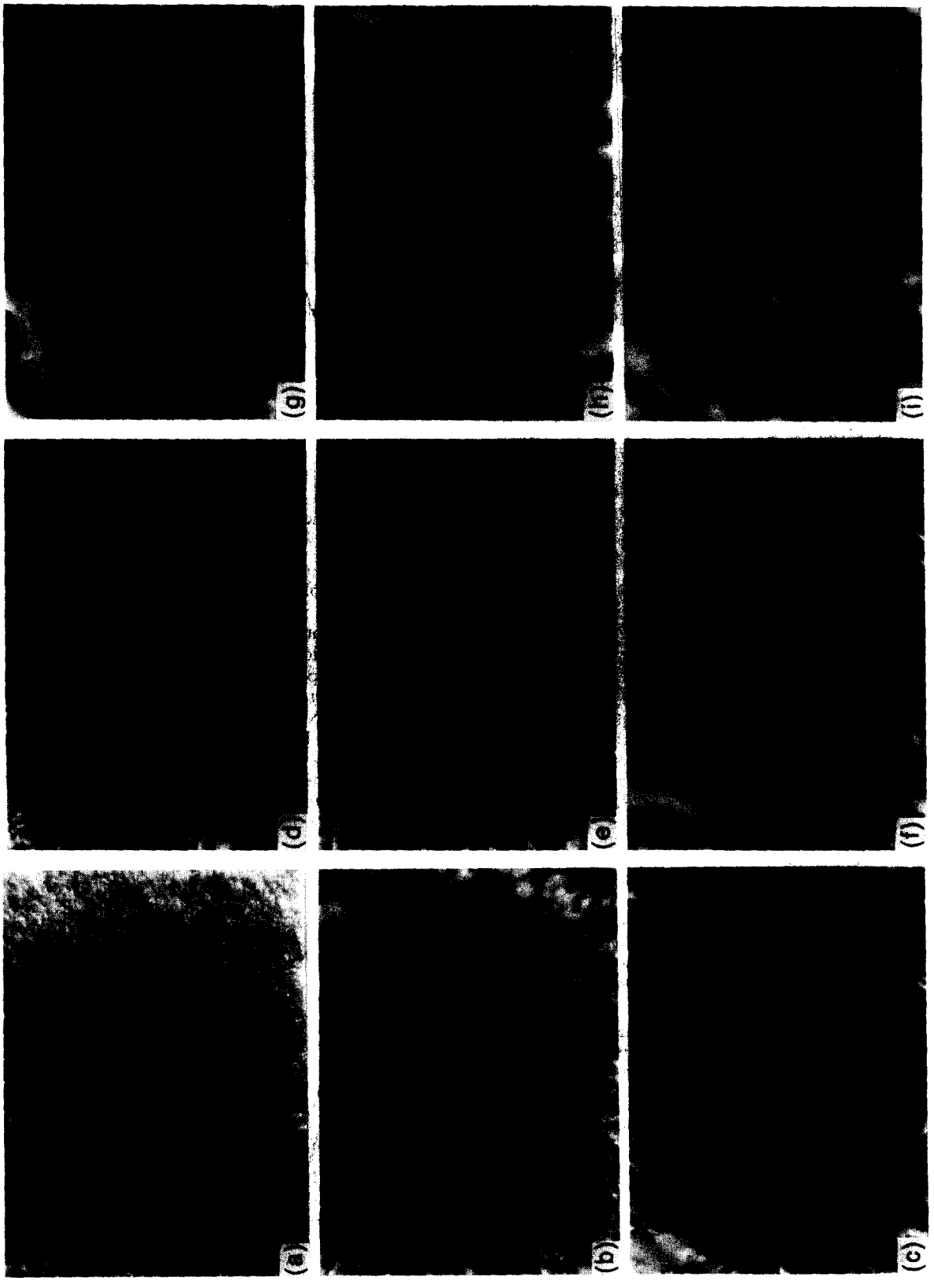

Fig. 1. Optical micrographs showing the blend morphology of different blend compositions. (a) N_{10}; (b) N_{20}; (c) N_{30}; (d) N_{40}; (e) N_{50}; (f) N_{60}; (g) N_{70}; (h) N_{80}; and (i) N_{90}.

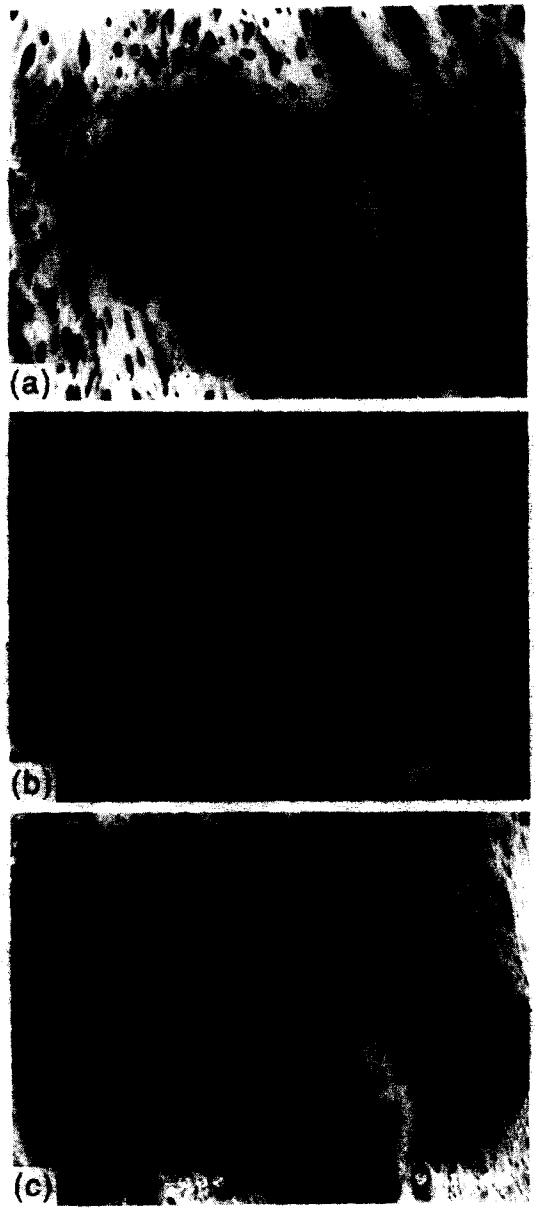

Fig. 2. SEMs. (a) Blend morphology of N_{30} showing the dispersed NBR particles in the continuous EVA matrix. (b) SEM of N_{50} showing a co-continuous morphology. (c) SEM showing the blend morphology of N_{70} where EVA particles are dispersed in NBR matrix.

using an Instron Universal Testing Machine (model 1121). The hardness of the samples was measured according to ASTM D-2240-86 and expressed in Shore A units.

Viscoelastic properties

The viscoelastic properties of the samples were measured using a Rheovibron DDV-III-C at a strain amplitude of 0.0025 cm and a frequency of 35 Hz. The temperatures of the testing were in the range of −120 to 80°C.

RESULTS AND DISCUSSION

Morphology of the blends

The major factors affecting blend morphology are volume fraction and viscosity. Danesi and Porter [42] have shown that for the same processing conditions

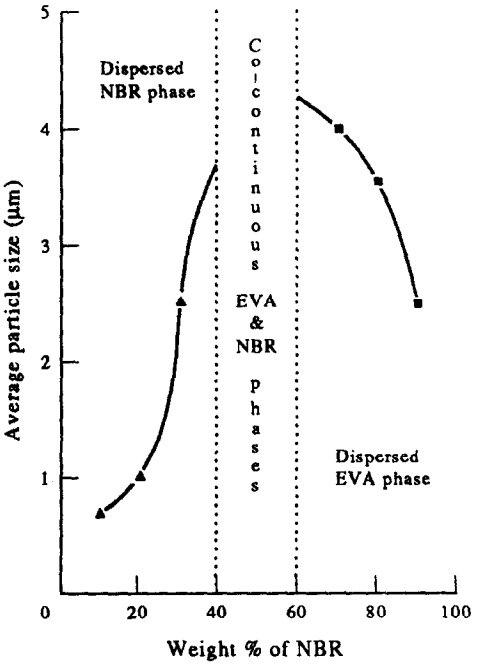

Fig. 3. Effect of blend composition on the dispersed particle size.

the blend morphology is determined by the composition ratio and melt viscosity differences of the components. Continuity of a phase is favoured by high volume fraction and low viscosity relative to that of the other component.

The optical micrographs of the blends are shown in Fig. 1. In N_{10}, N_{20} and N_{30} [Fig. 1(a–c)], NBR is dispersed in the EVA matrix. Correspondingly in N_{90}, N_{80}, and N_{70} [Fig. 1(i), (h) and (g)] EVA is the dispersed phase but with a larger domain size. This is due to the clustering of EVA domains as reported in the case of NR/EVA blends [13]. Occurrence of coalescence at higher concentrations of one of the components has been reported by many authors [32, 43–45]. In the case of polyethylene/polystyrene blends, the increase in domain dimension of PE at its higher concentration is caused by coalescence [43]. Thomas *et al.* [16, 44] have reported similar

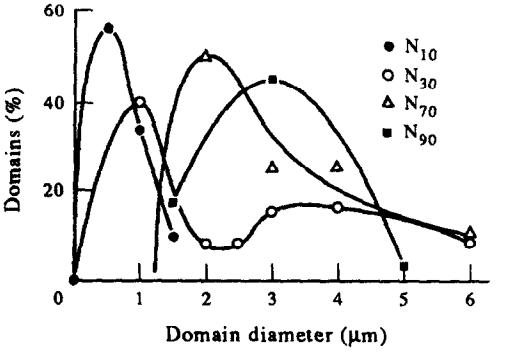

Fig. 4. Particle size distribution curve for the blend compositions N_{10}, N_{30}, N_{70} and N_{90}.

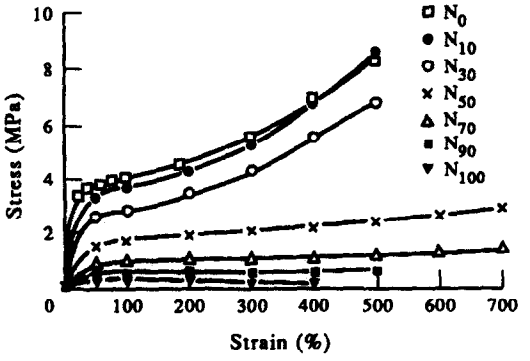

Fig. 5. Stress–strain behaviour of NBR/EVA blends with different blend ratio.

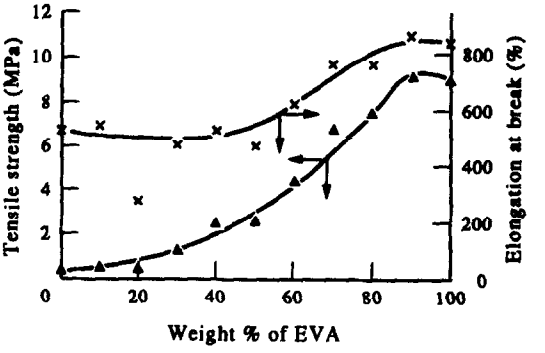

Fig. 7. Variation of tensile strength and elongation at break as a function of blend composition.

phenomenon in the case of hytrel/PVC and EVA/PP blends. In N_{40}, N_{50} and N_{60} [Fig. 1(d–f)] both the phases exist as continuous phases. The elongated nature of the dispersed particles in N_{30} is also observed in scanning electron micrograph. The SEM of some blend compositions are given in Fig. 2. In N_{30} and N_{70} [Fig. 2(a and c)] the minor NBR component is dispersed within a continuum of the major EVA component. N_{50} [Fig. 2(b)] is showing a co-continuous morphology where both the components are continuous. The average particle size vs blend composition is shown in Fig. 3. In the blends with high EVA content, NBR is the dispersed phase and the average particle size of the dispersed domains increase with the increase in NBR content. In the NBR rich blends the average particle size of the dispersed EVA domains increase with the increase in EVA content. The increase in domain size of EVA or NBR with increasing proportion of that component is associated with the coalescence or recombination of the domains [13, 32, 43–45]. Between 40 and 60 wt% of NBR a co-continuous morphology is exhibited. The particle size distribution curve (Fig. 4) is drawn by measuring the size of 100 particles from the optical micrographs. N_{90} is having a broader distribution curve than N_{10} which is as a result of the clustering of EVA particles.

Mechanical properties

The stress–strain curves of the samples are shown in Fig. 5. The differences in deformation characteristics of homopolymers and blends under an applied load are evident from the stress–strain curves. Pure

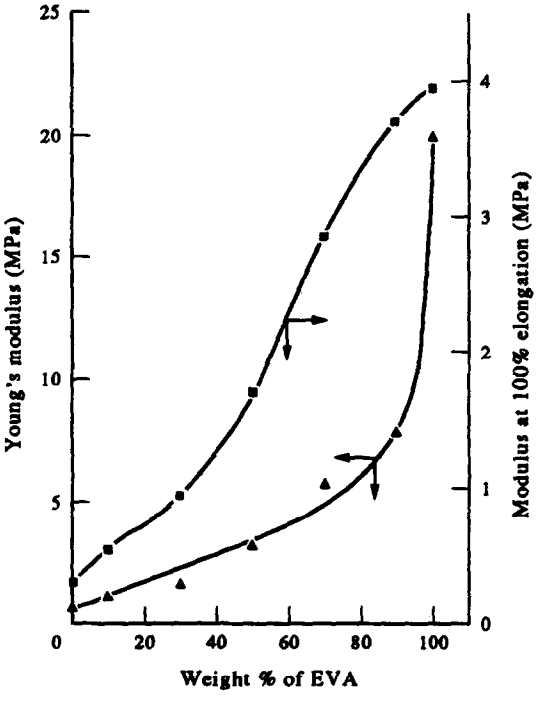

Fig. 6. Variation of Young's modulus and modulus at 100% elongation as a function of blend composition.

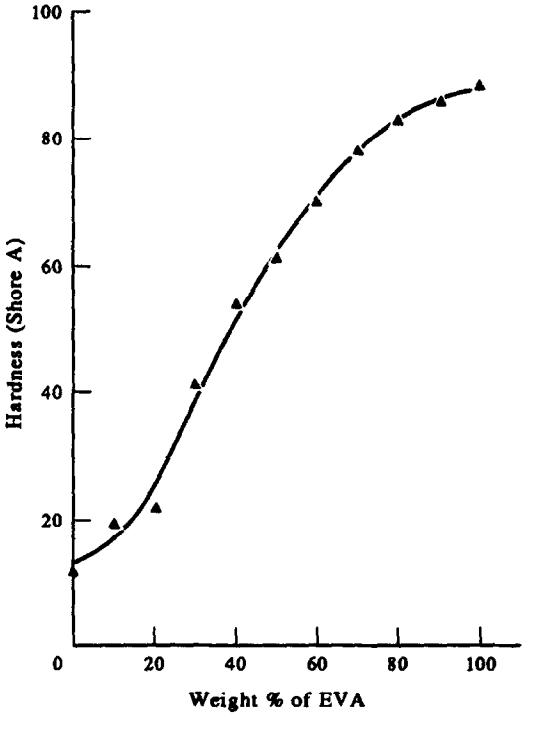

Fig. 8. Effect of blend composition on the hardness of the blends.

Table 2. Mechanical properties of NBR/EVA blends

Sample reference	Tensile strength (MPa)	Elongation at break (%)	Young's modulus (MPa)	(Hardness (Shore A)
N_0	8.79	843	20.00	89
N_{10}	9.24	864	7.86	86
N_{30}	6.83	769	5.71	79
N_{50}	2.83	429	3.20	62
N_{70}	1.29	487	1.67	41
N_{90}	0.53	494	1.13	19
N_{100}	0.35	535	0.65	12

Table 3. Viscoelastic properties of NBR/EVA blends

Sample reference	Tan δ Maximum	Tan δ Relative peak width at half height	Peak, T_g (°C)	E'' peak T_g (°C)
N_0	0.190	2.17	10	−21.0
N_{30}	0.345	1.58	−13	−21.5
N_{50}	0.490	1.33	14	−20.0
N_{70}	0.810	1.58	−12	−23.0
N_{100}	1.400	1.00	−10	−27.0

EVA and EVA rich blends show higher initial modulus with a yield point. At higher strains these blends show a gradual increase in stress which can be attributed to the orientation of the polyethylene crystalline hard segments of EVA, the continuous phase, in the direction of applied stress. The stress–strain curves of pure EVA and high EVA blends have distinct elastic and inelastic regions. In the inelastic region, the samples undergo yielding and strain induced crystallization. The stress–strain curve of NBR (N_{100}) is the typical one for uncrosslinked rubbers. In the blends N_{70} and N_{90} where NBR is the continuous phase a similar stress–strain behaviour as that of NBR is obtained. N_{50} with a co-continuous morphology shows a stress–strain behaviour which is intermediate between those of the other blend compositions.

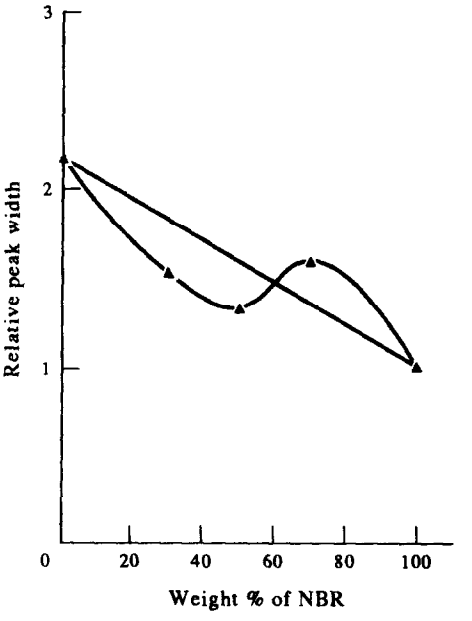

Fig. 10. Effect of blend composition on the relative tan δ peak width.

In Fig. 6 Young's modulus and modulus at 100% elongation are plotted as function of blend composition. Young's modulus of the blends increase with EVA content. The increase in modulus at 100% elongation is less marked at the extreme ends of the curve compared to the middle portion. Elongation at break, tensile strength and hardness increase with the weight percentage of EVA (Figs 7 and 8). In all these

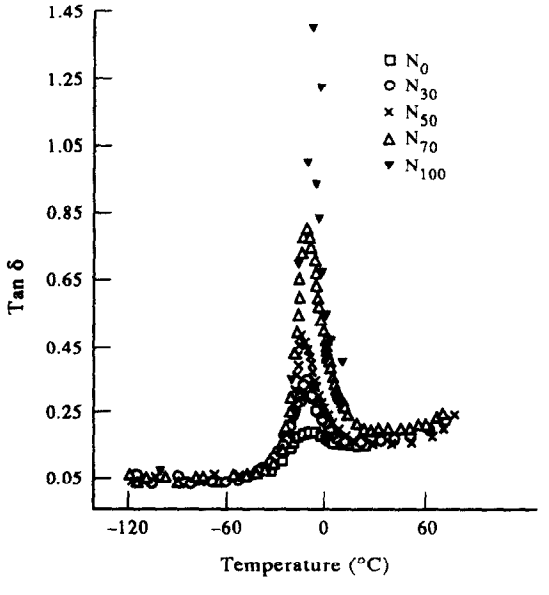

Fig. 9. Effect of temperature on the tan δ values of NBR/EVA blends.

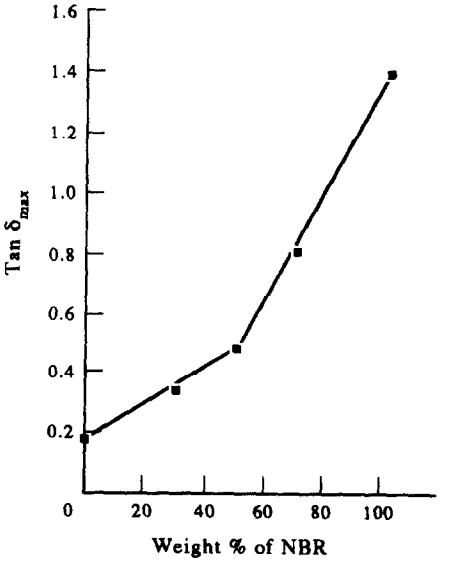

Fig. 11. Variation of tan δ_{max} with weight percentage of NBR.

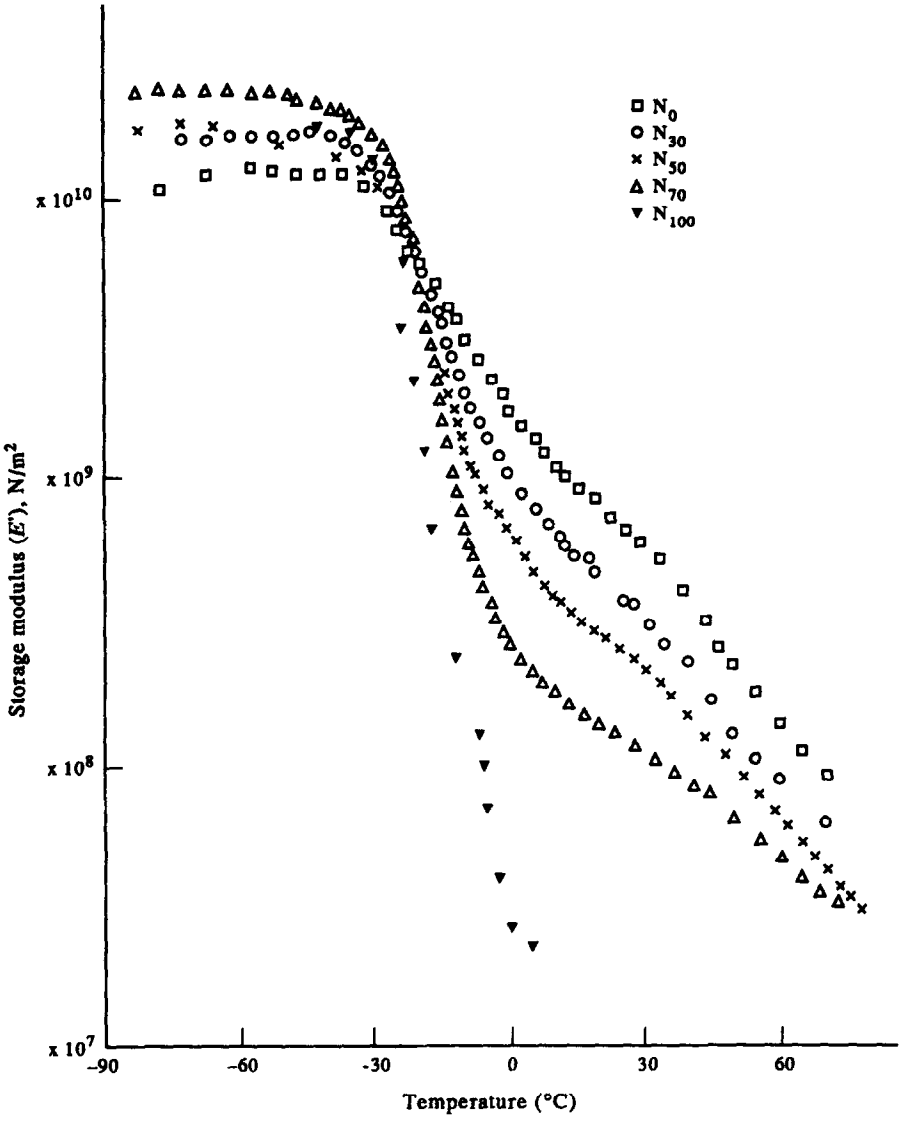

Fig. 12. Effect of temperature on the storage modulus of NBR/EVA blends.

curves the properties increase more sharply when the EVA content is more than 40%. This is due to the fact that when the weight percentage of EVA is more than 40%, it tends to become the continuous phase. The mechanical properties of these blends are given in Table 2.

Viscoelastic properties

Figure 9 shows the loss tangent (tan δ) values of the blends and homopolymers as a function of temperature. Nitrile rubber and EVA show the glass transitions at -10°C, i.e. glass transition temperatures of both the polymers are same. In the case of blends there is a single, sharp transition which shifts slightly towards the lower temperature region with blend ratio. However, miscibility cannot be ascertained by the T_g measurements since the glass transition of both the components are at the same temperature. The peak width at half height of the tan δ curve is measured and given in Table 3. It is seen that the peak widths of the blends take intermediate values between those of the pure components, i.e. some variations in broadening of the glass transition zone with respect to blend composition. The relative peak width of tan δ curve against blend composition is plotted in Fig. 10. The curve shows positive and negative deviation depending on the composition. A similar variation is reported by Varghese *et al.* [46] for miscible blends from plasticized poly(vinyl chloride) and epoxidized natural rubber. This indicates some marginal level of compatibility in some of the blend compositions. Figure 11 is a graph showing the variation of tan δ_{max} with the weight percentage of NBR. It can be noticed that the damping properties of the blends increase with increasing nitrile rubber content. The tan δ_{max} values show a regular increase up to 50% of NBR followed by a sharp increase at higher content of NBR. This is due to the fact that

there occurs a phase inversion in the morphology of the blend from N_{50} onwards. This is clearly evident from the SEMs.

The influence on temperature on the storage modulus of the samples is shown in Fig. 12. The curves for all the compositions have three distinct regions: a glassy region, a transition region and a rubbery region. Blends with higher proportions of NBR show higher values of storage moduli at lower temperatures (below $-20°C$). But at higher temperatures the trend is reversed which is evident from the lower modulus of NBR rich samples. Interestingly all the curves intersect around the glass transition region of the blends. At higher temperatures (above T_g) NBR changes from glassy state to amorphous state. Also on increasing the NBR content the crystallinity is reduced. Therefore the modulus of NBR rich blends decrease at higher temperatures. A similar trend is reported in the case of miscible hytrel/PVC blends by Thomas *et al.* [44]. In the plot of loss modulus (E'') against temperature there is also a similar behaviour as in the case of storage modulus curve observed around the glass transition region (Fig. 13). Below glass transition region ($T < T_g$) NBR rich blends show higher values of loss modulus. As the temperature is increased and the EVA rich blends exhibit higher loss modulus. The T_g values obtained from E'' vs temperature plots are always lower than those obtained from tan δ_{max} values (Table 3). The storage and loss modulus at 0°C as a function of wt% of NBR is presented in Fig. 14. It is seen that both storage and loss moduli decrease with the increase of NBR content.

Reprocessability/degradation of the material

One of the important advantages of thermoplastic elastomer is their recyclability and reprocessability. The recyclability of the blends has been analysed by

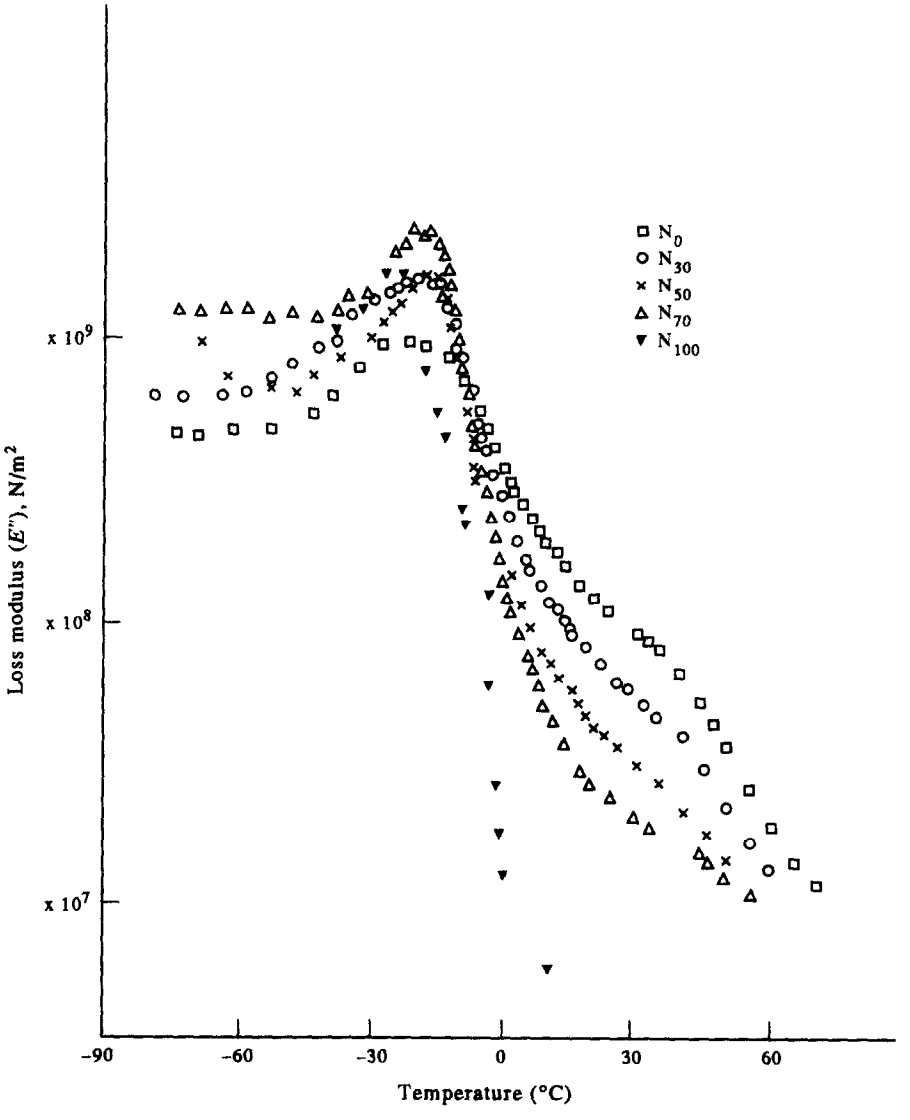

Fig. 13. Effect of temperature on the loss modulus of NBR/EVA blends.

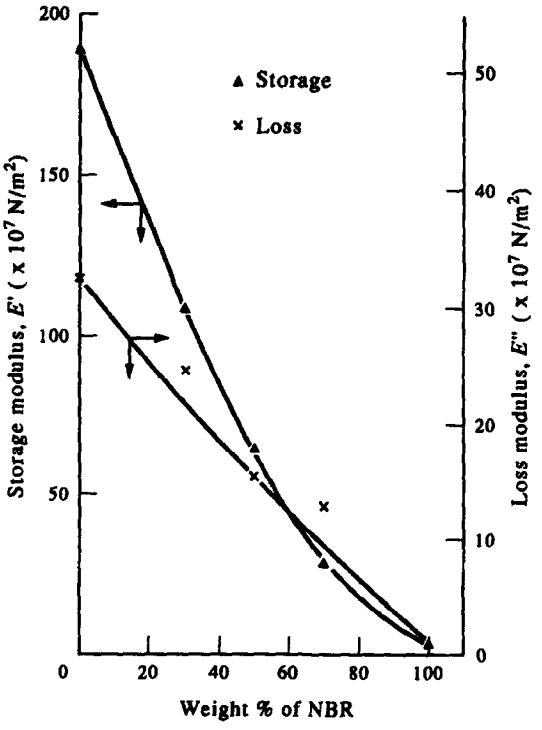

Fig. 14. Variation of storage and loss moduli with blend composition at 0°C.

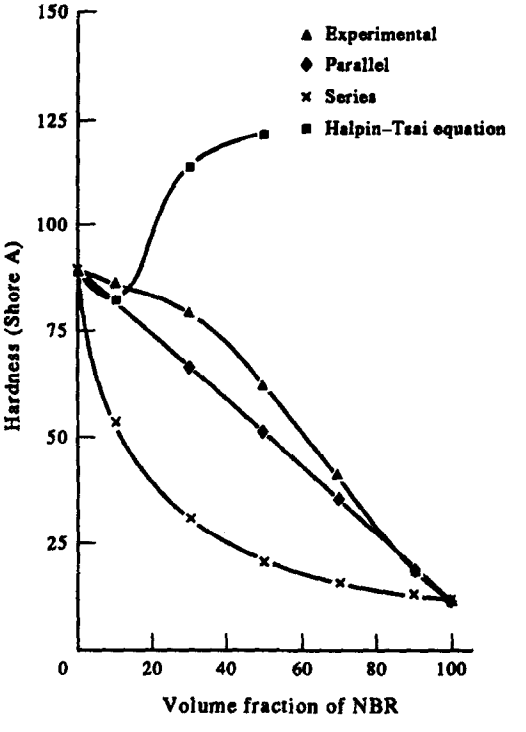

Fig. 16. Applicability of various models on hardness of the blends.

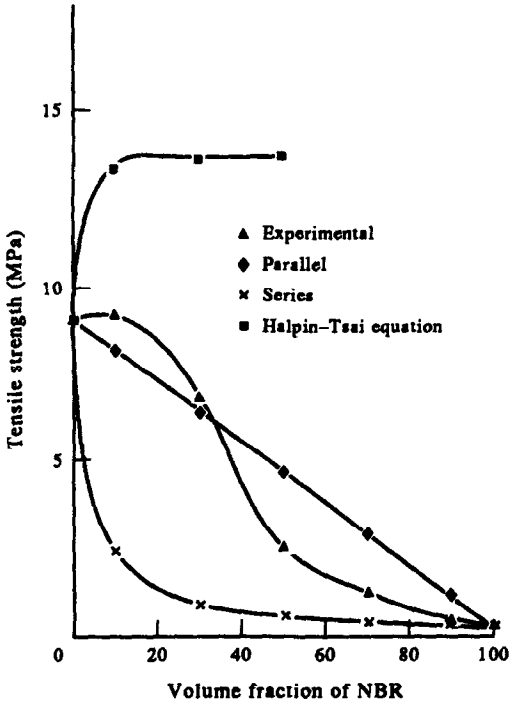

Fig. 15. Applicability of various models on tensile strength of the blends.

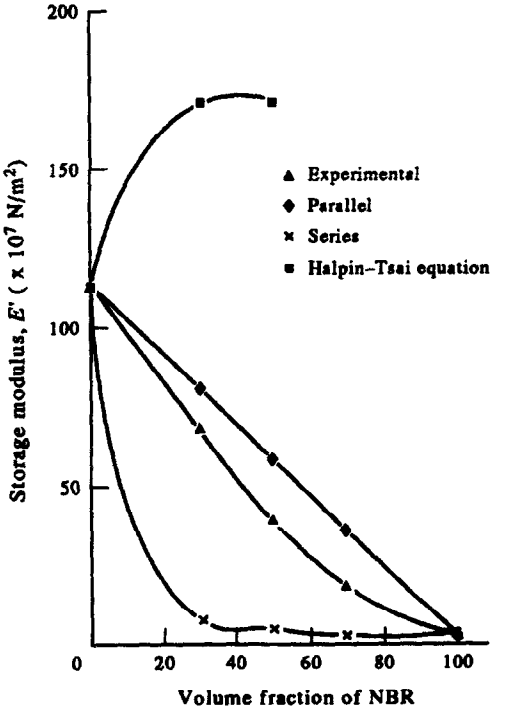

Fig. 17. Applicability of various models on storage modulus of the blends at 10°C.

repeated moulding (four times) at 150°C. The properties of the recycled blends have been measured. It is interesting to note that the properties of the recycled blends remain constant. This indicates that there was no substantial degradation during processing of these blends. However, this is a subject of our future publication.

Model fitting

Applicability of various composite models such as the parallel model, series model and Halpin–Tsai equation [47, 48] have been examined to predict the mechanical and viscoelastic behaviour of these blends. The upper bound of modulus is given by the rule of mixtures

$$M = M_1\phi_1 + M_2\phi_2 \quad (1)$$

where M is the modulus of the blend, M_1 and M_2 are the moduli of the components 1 and 2 respectively, ϕ_1 and ϕ_2 are the volume fraction of the components 1 and 2 respectively. This equation is applicable for models in which the components are arranged parallel to the applied stress. The lower bound of the modulus holds models in which the components are arranged in series with the applied stress and the equation is

$$1/M = \phi_1/M_1 + \phi_2 M_2. \quad (2)$$

According to Halpin–Tsai equation

$$M_1/M = (1 + A_i B_i \phi_2)/(1 - B_i\phi_2) \quad (3)$$

$$B_i = (M_1/M_2 - 1)/(M_1/M_2 + A_i). \quad (4)$$

In the Halpin–Tsai equation subscripts 1 and 2 refer to the continuous and dispersed phase respectively. The constant A_i is defined by the morphology of the system. For elastomer domains dispersed in a continuous hard matrix, $A_i = 0.66$. The applicability of these models to mechanical and viscoelastic properties is presented in Figs 15–17. In all cases it is seen that the experimental data are close to the parallel model.

CONCLUSION

The morphology of NBR/EVA blends indicates a two phase structure in which the minor component is dispersed within a continuum of the major component. A co-continuous morphology was obtained when the NBR content was between 40–60%. The mechanical properties such as tensile strength, elongation at break and hardness increase with the increase in EVA content. The increase was sharper when the EVA content was more than 40% where it formed a continuous phase. The stress–strain curves of EVA rich blends have a similar behaviour as that of pure EVA, NBR rich blends as that of pure NBR and the 50/50 blend with a co-continuous morphology showed an intermediate stress–strain behaviour. The viscoelastic behaviour of these blends have been studied with special reference to the effects of blend ratio and temperature. At lower temperatures (below T_g) NBR rich blends showed higher values of storage moduli because of its glassy nature below glass transition temperature. But the trend is reversed at higher temperatures. This is due to the higher proportion of NBR in the blends which is in its amorphous state at higher temperatures (above T_g). The damping properties of the blends decreased with the increase of EVA content. The changes in dynamic properties could be related to the morphology of the system. All the blends showed a single glass transition temperature. However, miscibility of the system cannot be ascertained by this technique since the glass transition temperature of both the pure components are at the same temperature. Various theoretical models have been used to predict the mechanical and viscoelastic behaviour of these blends. It was found that the experimental results could be predicted by the parallel model.

Acknowledgements—The authors are grateful to Mr Filcy T. Baby, Botany Department, CMS College, Kottayam for his assistance given for carrying out the optical analysis of the blends.

REFERENCES

1. In *Encyclopedia of Polymer Science and Engineering*, Vol. 12, p. 399. Wiley, New York (1988).
2. D. R. Paul and J. O. Altamirano. *Adv. chem. Ser.* **142,** 371 (1975).
3. R. L. Imken, D. R. Paul and J. W. Barlow. *Polym. Engng Sci.* **16,** 593 (1976).
4. R. E. Bernstein, D. R. Paul and J. W. Barlow. *Polym. Engng Sci.* **18,** 683 (1978).
5. R. E. Bernstein, C. A. Cruz, D. R. Paul and J. W. Barlow. *Macromolecules* **10,** 681 (1977).
6. D. R. Paul, J. W. Barlow, C. A. Cruz, R. N. Mohan, T. R. Nassar and D. C. Wahrmund. *Am. chem. Soc., Div. Organ. Coat. Plast. Chem.* **37,** 130 (1977).
7. L. P. McMaster. *Adv. chem. Ser.* **142,** 43 (1975).
8. L. P. McMaster. *Macromolecules* **6,** 760 (1973).
9. T. K. Kwei, T. Nishi and R. F. Roberts. *Macromolecules* **7,** 667 (1974).
10. R. Greco, E. Martuscelli, G. Ragosta and Yin Jinghusa. *J. Mater. Sci.* **23,** 4307 (1988).
11. N. Roychoudhury and A. K. Bhowmick. *Polym. Degrad. Stabil.* **25,** 39 (1989).
12. S. S. Bhagawan, D. K. Tripathy and S. K. De. *J. Mater. Sci. Lett.* **6,** 157 (1987).
13. A. T. Kozhy. Ph.D thesis submitted to Mahatma Gandhi University (1991).
14. X. Zhang and Y. Zhang. In *Proc. Int. Rubber Conf.*, p. 29. RUBBERCON '93, New Delhi (1993).
15. I. Ray, D. Khastgir and P. G. Mukunda. *Die. Angew. Markromol. Chem.* **205,** 59 (1993).
16. S. Thomas, S. K. De and B. R. Gupta. *Kautsch. Gummi Kunst.* **40,** 7, 665 (1987).
17. M. K. Ghosh, S. K. Singha Roy and C. K. Das. In *Proceedings of International Rubber Conference*, p. 137. RUBBERCON '93, New Delhi (1993).
18. A. Y. Coran, R. Patel and D. Williams-Headd. *Rubb. chem. Technol.* **58,** 1014 (1985).
19. A. Y. Coran, R. Patel and D. Williams-Headd. *Rubb. chem. Technol.* **55,** 116 (1982).
20. E. E. C. Montein and C. Thaumaturgo. *Polym. Bull.* **30,** 696 (1993).
21. M. L. Addonizio, L. D'Orazio, C. Mancarella and E. Martuscelli. *J. Mater. Sci.* **24,** 2939 (1989).
22. D. Hay, H. A. Pfisterer and E. B. Storey. *Rubb. Age* **94,** 77 (1955).
23. N. B. Fegade, N. A. Phondke and W. Millns. In *Proceedings of International Rubber Conference*, p. 43. RUBBERCON '93, New Delhi (1993).
24. A. Y. Coran and R. Patel. *Rubber Chem. Technol.* **56,** 1045 (1983).

25. S. Thomas, B. R. Gupta and S. K. De. *Polym. Degrad. Stab.* **18,** 189 (1987).
26. S. Thomas, B. R. Gupta and S. K. De. *J. Mater. Sci.* **22,** 3209 (1987).
27. S. Thomas, B. Kuriakose, B. R. Gupta and S. K. De. *Plast. Rubb. Process. Applic.* **6,** 101 (1986).
28. S. Thomas. *Mater. Lett.* **5,** 9 (1987).
29. A. T. Koshy, B. Kuriakose and S. Thomas. *Ind. J. Nat. Rubb. Res.* **3,** 77 (1990).
30. A. T. Koshy, B. Kuriakose, S. Thomas and S. Varghese. *Polymer* **34,** 3428 (1993).
31. A. T. Koshy, B. Kuriakose, S. Thomas, C. K. Premalatha and S. Varghese. *J. appl. Polym. Sci.* **49,** 901 (1993).
32. K. C. Dao. *Polymer* **25,** 1527 (1984).
33. M. Baer. *J. appl. Polym. Sci.* **16,** 1109 (1972).
34. C. K. Riew, E. H. Rowe and A. R. Siebert. In *Advances in Chemistry*, Series 154. Am. Chem. Soc. Washington, D.C. (1976).
35. S. Cimmino, L. D'orazio, R. Greco, G. Maglio, M. Malinconico, C. Mancarella, E. Martuscelli, R. Palumbo and G. Ragosta. *Polym. Engng Sci.* **24,** 48 (1984).
36. D. Yang, B. Zhang, Y. Yang, Z. Fang, G. Sun and Z. Feng. *Polym. Engng Sci.* **24,** 612 (1984).
37. G. N. Avgeropoulos, F. C. Weissert and G. G. A. Bohm. *Rubb. Chem. Technol.* **49,** 93 (1976).
38. R. J. Spontak, S. D. Smith and A. Ashraf. *Macromolecules* **26,** 956 (1993).
39. R. Greco, C. Mancarella, E. Martuscelli, G. Ragosta and Yin Jinghua. *Polymer* **28,** 1929 (1987).
40. S. Akhtar, P. P. De and S. K. De. *J. appl. Polym. Sci.* **32,** 5123 (1986).
41. O. Olabisi, L. M. Robeson and M. T. Shaw (Eds). In *Polymer–Polymer Miscibility*. Academic Press, London (1979).
42. S. Danesi and R. S. Porter. *Polymer* **19,** 448 (1978).
43. D. Heikens and W. Barentsen. *Polymer* **18,** 69 (1977).
44. S. Thomas, B. R. Gupta and S. K. De. *J. Vinyl Technol.* **9,** 71 (1987).
45. Z. K. Walczak. *J. appl. Polym. Sci.* **17,** 169 (1973).
46. K. T. Varghese, P. P. De, S. K. Sanyal and S. K. De. *J. appl. Polym. Sci.* **37,** 2537 (1989).
47. S. Thomas and A. George. *Eur. Polym. J.* **28,** 1451 (1992).
48. L. E. Nielsen. *Rheol. Acta.* **13,** 86 (1974).